

Very Large Excesses of ^{18}O in Hydrogen-Deficient Carbon and R Coronae Borealis Stars: Evidence for White Dwarf Mergers

Geoffrey C. Clayton¹, T.R. Geballe², Falk Herwig^{3,4}, Christopher Fryer⁴, and Martin Asplund⁵

ABSTRACT

We have found that at least seven hydrogen-deficient carbon (HdC) and R Coronae Borealis (RCB) stars, have $^{16}\text{O}/^{18}\text{O}$ ratios close to and in some cases less than unity, values that are orders of magnitude lower than measured in other stars (the Solar value is 500). Greatly enhanced ^{18}O is evident in every HdC and RCB we have measured that is cool enough to have detectable CO bands. The three HdC stars measured have $^{16}\text{O}/^{18}\text{O} < 1$, lower values than any of the RCB stars. These discoveries are important clues in determining the evolutionary pathways of HdC and RCB stars, for which two models have been proposed: the double degenerate (white dwarf (WD) merger), and the final helium-shell flash (FF). No overproduction of ^{18}O is expected in the FF scenario. We have quantitatively explored the idea that HdC and RCB stars originate in the mergers of CO- and He-WDs. The merger process is estimated to take only a few days, with accretion rates of $150\text{ M}_{\odot}\text{ yr}^{-1}$ producing temperatures at the base of the accreted envelope of $1.2\text{--}1.9 \times 10^8\text{ K}$. Analysis of a simplified one-zone calculation shows that nucleosynthesis in the dynamically accreting material may provide a suitable environment for a significant production of ^{18}O , leading to very low values of $^{16}\text{O}/^{18}\text{O}$, similar to those observed. We also find qualitative agreement with observed values of $^{12}\text{C}/^{13}\text{C}$ and with the CNO elemental ratios. H-admixture during the accretion process from the small H-rich C/O WD envelope may play an important role in producing the observed abundances. Overall our analysis

¹Department of Physics & Astronomy, Louisiana State University, Baton Rouge, LA 70803; gclayton@fenway.phys.lsu.edu

²Gemini Observatory, 670 N. A'ohoku Place, Hilo, HI 96720; tgeballe@gemini.edu

³Keele Astrophysics Group, School of Physical and Geographical Sciences, Keele University, Staffordshire ST5 5BG, UK; fherwig@astro.keele.ac.uk

⁴Los Alamos National Laboratory, Los Alamos, NM 87545; clfreyer@lanl.gov

⁵Research School of Astronomy and Astrophysics, Mount Stromlo Observatory, Cotter Road, Weston, ACT 2611, Australia; martin@mso.anu.edu.au

shows that WD mergers may very well be the progenitors of O¹⁸-rich RCB and HdC stars, and that more detailed simulations and modeling are justified.

Subject headings: stars: evolution — stars: abundances — stars: AGB and post-AGB — stars: variables: R Coronae Borealis

1. Introduction

Among the hydrogen-deficient post-asymptotic giant branch (post-AGB) stars are the R Coronae Borealis (RCB) stars, a small group of carbon-rich supergiants. About 50 RCB stars are known in the Galaxy and the Magellanic Clouds (Kraemer et al. 2005; Zaniewski et al. 2005; Alcock et al. 2001; Clayton 1996). Their defining characteristics are hydrogen deficiency and unusual variability - RCB stars undergo massive declines of up to 8 mag due to the formation of carbon dust at irregular intervals. Apparently related to the RCB stars are the hydrogen-deficient carbon (HdC) stars. The five known HdC stars are similar to the RCB stars spectroscopically but do not show declines or IR excesses (Warner 1967).

Two scenarios have been proposed for the origin of an RCB star: the double degenerate (DD) and the final helium-shell flash (FF) models (Iben et al. 1996; Saio & Jeffery 2002). The former involves the merger of a CO- and a He-white dwarf (WD) (Webbink 1984). In the latter, thought to occur in 20% of all AGB stars, a star evolving into a planetary nebula (PN) central star is blown up to supergiant size by a FF (Fujimoto 1977; Renzini 1979). Three stars (Sakurai’s Object, V605 Aql, and FG Sge) have been observed to undergo FF outbursts that transformed them from hot evolved PN central stars into cool giants with spectral properties similar to RCB stars (Asplund et al. 1998, 1999, 2000; Clayton & De Marco 1997; Gonzalez et al. 1998). In two of these, Sakurai’s Object and V605 Aql, the FFs are thought to be the result of Very Late Thermal Pulses (VLTPs)¹, FFs that occur on the WD cooling track (e.g., Herwig 2001), because their post-outburst evolutions have been so rapid and because in some cases an ionized nebula was found surrounding the cool post-outburst object (Ford 1971; Duerbeck & Benetti 1996). V605 Aql has evolved from $T_{eff}=5000$ K in 1921 (two years after its outburst) to 95,000 K today (Clayton et al. 2006) and now has abundances similar to those seen in Wolf-Rayet [WC] central stars of PNe, with 55% He, and 40% C, and not similar to those seen in the RCB and HdC stars. Sakurai’s Object became enshrouded in dust three years after its outburst, and thus most of its current stellar properties cannot be

¹FG Sge is thought to be the result of a Late Thermal Pulse (LTP) and is not considered further here (Herwig 2001).

determined. However, just after their outbursts, both V605 Aql and Sakurai’s Object were almost indistinguishable from the RCB stars, in abundances (except for the presence of ^{13}C), temperature, and absolute luminosity. Nevertheless, the very short observed timescales for this RCB-like phase make it unlikely that objects such as these can account for even the small number of RCB stars known in the Galaxy (Clayton et al. 2006).

Recently, Clayton et al. (2005) discovered that $^{16}\text{O}/^{18}\text{O} \lesssim 1$ in the HdC star, HD 137613, from a spectrum of the first overtone bands of CO at 2.3-2.4 μm . As the bands of $^{12}\text{C}^{16}\text{O}$ are of typical strength for a cool star, the measured ratio implies a huge enhancement of ^{18}O rather than a depletion of ^{16}O . The isotopic ratio is orders of magnitude less than that measured in other stars (Clayton et al. 2005). The value of $^{16}\text{O}/^{18}\text{O}$ is ~ 500 in the solar neighborhood (Scott et al. 2006; Geiss et al. 2002) and varies from 200 to 600 in the Galactic interstellar medium (Wilson & Rood 1994). Only one other star, the post-AGB star HR 4049, has been found to have highly enhanced ^{18}O (Cami & Yamamura 2001). HR 4049 is a binary and its enhanced oxygen isotopes ($^{16}\text{O}/^{18}\text{O} \approx 7$ and $^{16}\text{O}/^{17}\text{O} \approx 8$) are found in the circumbinary disk material. High abundances of ^{18}O have also been measured in pre-solar graphite grains in the Murchison meteorite (Amari et al. 1995) and are attributed to material processed in massive Wolf-Rayet stars. In both of these other cases (HR 4049 and meteorites), the abundance of ^{18}O relative to ^{16}O is several times less than in HD 137613.

In this paper, we analyze new high S/N spectra of the K-band CO bands in HD 137613 and nine additional RCB and HdC stars to investigate $^{16}\text{O}/^{18}\text{O}$ in these stars. The sample includes all known HdC stars and five RCB stars cool enough to have prominent CO bands. Clayton et al. (2005) discussed the failure of several nucleosynthesis scenarios to explain the unusually small $^{16}\text{O}/^{18}\text{O}$ ratio in HD 137613. In the light of the new observations, we explore the idea that HdC and RCB stars originate in DD mergers of a CO and a He-WD. We first investigate whether the conditions exist in a WD merger for nucleosynthesis to take place and then estimate the results of the nucleosynthesis.

2. Observations and Data Reduction

We obtained a more extensive K-band spectrum of HD 137613 than the one published by Clayton et al. (2005) on UT 2005 March 04 at the 3.8 m United Kingdom Infrared Telescope (UKIRT). The new observation used the facility instrument UIST with its long K grism and $0''.24$ (2 pixel-wide) slit to cover 2.20-2.51 μm at a resolving power of ~ 3500 (Ramsay Howat et al. 2004). Standard observing and reduction techniques were employed. A wavelength calibration accuracy of better than 0.0001 μm was achieved using the spectrum of an argon arc lamp. The calibration star used to remove telluric absorption lines and flux-

calibrate the spectrum of HD 137613 was HR 5514 (B9V). The reduced spectrum is plotted in Fig. 1, with vertical lines indicating the bandhead wavelengths. It shows, in addition to the 2-0, 3-1, and 4-2 bands of $^{12}\text{C}^{18}\text{O}$ discovered by Clayton et al. (2005), the 5-3, 6-4, and 7-5 bands. In addition to the six bands of $^{12}\text{C}^{18}\text{O}$, at least seven and probably eight bands of $^{12}\text{C}^{16}\text{O}$ are seen. As in the previously published K-band spectrum of HD 137613 the strengths of the $^{12}\text{C}^{18}\text{O}$ and $^{12}\text{C}^{16}\text{O}$ bands are approximately equal, implying near equal abundances of the two isotopomers. The spectrum shows no evidence for either $^{13}\text{C}^{16}\text{O}$ or $^{12}\text{C}^{17}\text{O}$.

The Gemini-S facility spectrometer, GNIRS was employed on UT 2005 September 26-28 to obtain spectra of nine HdC and RCB stars. The spectrograph was used in the short camera mode and with the $0''.3$ (2 pixel-wide) slit to cover 2.27 to 2.51 μm at $R=5900$. The observations were reduced by dividing the spectrum of each RCB and HdC star by that of a nearby bright early A-type dwarf star to remove the instrumental response and the effects of atmospheric absorption lines. Wavelength calibration was obtained from these telluric lines and is accurate to better than 0.0001 μm .

The complete observing sample is listed in Table 1 and the 2.28–2.45 μm portions of the spectra are plotted in Fig. 2. Also included is the previously published spectrum of the RCB star, Z UMi (Tenenbaum et al. 2005). The wavelengths of the bandheads of $^{12}\text{C}^{16}\text{O}$ and $^{12}\text{C}^{18}\text{O}$ are indicated by vertical lines. The signal-to-noise ratios of the spectra are 100 or more. The spectra have been shifted to correct for the stars’ measured heliocentric radial velocities (Lawson & Cottrell 1997; Duffot et al. 1995; Goswami et al. 1997). One star, ES Aql, does not have a published radial velocity. We have estimated it to be $\sim 55 \text{ km s}^{-1}$ and made the correction in Fig. 2.

3. Preliminary Results

Seven of the eleven stars in Fig. 2 show, in addition to prominent bands of $^{12}\text{C}^{16}\text{O}$, compelling evidence for bands of $^{12}\text{C}^{18}\text{O}$. These are the HdC stars HD 137613, HD 175893, and HD 182040, and the RCB stars WX CrA, ES Aql, S Aps, and SV Sge. One additional RCB star that we observed, U Aqr, shows marginal evidence for $^{12}\text{C}^{18}\text{O}$. We also find marginal evidence for $^{12}\text{C}^{18}\text{O}$ in the the spectrum of the RCB star, Z UMi (Tenenbaum et al. 2005).

In the spectra of three of the HdC stars, HD 137613 and HD 175893, and HD 182040, and in the spectrum of one RCB star, WX CrA, the $^{12}\text{C}^{18}\text{O}$ bands are about as strong or stronger than the $^{12}\text{C}^{16}\text{O}$ bands. The most remarkable case is the HdC star HD 175893, for which the maximum depths of the bands of $^{12}\text{C}^{18}\text{O}$ are more than twice as deep as those of $^{12}\text{C}^{16}\text{O}$.

The least secure of these four cases is the HdC star HD 182040, because the bands are weak, but there is accurate wavelength correspondence between observed absorption maxima and their expected wavelengths. As in the case of HD 175893, the $^{12}\text{C}^{18}\text{O}$ bands in its spectrum are noticeably stronger than the $^{12}\text{C}^{16}\text{O}$ bands. For the third HdC star, HD 137613, the $^{12}\text{C}^{18}\text{O}$ bands appear to be slightly stronger than the $^{12}\text{C}^{16}\text{O}$ bands, whereas in the RCB star with the strongest $^{12}\text{C}^{18}\text{O}$, WX CrA, the band strengths do not exceed those of $^{12}\text{C}^{16}\text{O}$. In three other RCB stars, ES Aql, S Aps, and SV Sge, the $^{12}\text{C}^{18}\text{O}$ bands are prominent, but are considerably weaker than the $^{12}\text{C}^{16}\text{O}$ bands. Two HdC stars, HD 148839 and HD 173409, have no significant CO bands, presumably because their relatively high photospheric temperatures preclude the formation of detectable amounts of CO. Thus for them no determinations of the relative abundances of the CO isotopomers are possible.

For the sources with weaker absorptions (U Aqr, Z UMi, and HD 182040), there is some possibility that the features at the expected wavelengths of the $^{12}\text{C}^{18}\text{O}$ bandheads are due to some other species (e.g., CN). However, the accurate wavelength agreement of the $^{12}\text{C}^{18}\text{O}$ bandheads (in terms both of absolute wavelength and wavelength difference from nearby $^{12}\text{C}^{16}\text{O}$ bandheads), plus the fact that the absorptions at those wavelengths are among the strongest (apart from the $^{12}\text{C}^{16}\text{O}$ absorptions) in each spectrum gives us confidence, especially in the case of HD 182040, that we are detecting $^{12}\text{C}^{18}\text{O}$. None of the spectra show evidence for absorption bands of $^{13}\text{C}^{16}\text{O}$, which are present in the spectra of some carbon stars. Very high $^{12}\text{C}/^{13}\text{C}$ ratios are one of the trademarks of the RCB and HdC stars (Alcock et al. 2001; Clayton 1996; Warner 1967).

4. Estimates of $^{16}\text{O}/^{18}\text{O}$

To further confirm the identification of the $^{12}\text{C}^{18}\text{O}$ bands in our sample and to provide a way to roughly estimate $^{16}\text{O}/^{18}\text{O}$, we have computed MARCS model atmosphere spectra for different CO isotopic abundances (Asplund et al. 1997). We ran a grid of models with the stellar parameters $T_{\text{eff}} = 5000, 5500, 6000$ K and $\log g = 1.5$ [cgs] and a chemical composition typical of RCB stars (Asplund et al. 1997). Values of $^{16}\text{O}/^{18}\text{O}$ chosen were, 0, 0.1, 0.33, 1, 3, 10, and infinity (no ^{18}O). Models with no CO were also run.

The spectra in Figs. 1 and 2 and the MARCS model spectra are complex, because, in addition to CO, other species that are abundant in carbon stars absorb strongly in the observed wavelength interval, as discussed by Clayton et al. (2005). In order to estimate the $^{16}\text{O}/^{18}\text{O}$ ratio for each star we first need to measure the absorption depths of the $^{12}\text{C}^{16}\text{O}$ and $^{12}\text{C}^{18}\text{O}$ 2-0 and 3-1 bands. To do this, we started by binning the spectra in Fig. 2 and the MARCS spectra in intervals of $0.0005 \mu\text{m}$. From the MARCS spectra with no CO, we then

identified wavelength bins in the “continuum” just shortward and longward of each bandhead where absorption by other species is relatively weak. The ratios of the flux densities at the bandheads to the average of those at the “continuum” wavelengths, corrected for the net absorptions at the bandheads in the MARCS spectrum with no CO, are shown in the fourth column of Table 2 and provide a first estimate of the isotopic ratio $^{16}\text{O}/^{18}\text{O}$. The values shown are probably overestimates of this ratio where $^{16}\text{O}/^{18}\text{O} < 1$ and underestimates where $^{16}\text{O}/^{18}\text{O} > 1$, because the bands of the more abundant isotopomer are more saturated.

We have interpolated between the MARCS spectra to estimate the $^{16}\text{O}/^{18}\text{O}$ ratio for each star. The values are given in the right hand column of Table 2, and confirm the very low ratios in seven stars. However, the complexities of the observed and model spectra make determination of the isotopic ratios problematical, especially in cases such as this, where individual lines are not resolved. The MARCS spectra do not match the observed spectra in detail, adding to the uncertainties. We believe that the derived strengths of the 2-0 bandhead of $^{12}\text{C}^{18}\text{O}$ are more reliable than those of the 3-1 bandhead, where the correction for contaminating species was largest, and so we have weighted the ratios of the 2-0 band strengths more highly. Finally, the depths of the CO features in S Aps and SV Sge are greater than those in any of the model spectra that we generated; for these two stars, we used the 5000 K MARCS models. For all of these reasons we estimate the uncertainties in the derived isotopic ratios to be accurate only to a factor of two.

5. Discussion

In a prescient paper, Warner (1967) predicted that HdC stars would be rich in ^{18}O . He noted that just before He burning begins in the core of an intermediate mass star the temperature increases to values where $^{14}\text{N}(\alpha, \gamma)^{18}\text{F}(\beta^+ \nu)^{18}\text{O}$ can occur and subsequently the outer envelope of the star is lost through nova- or PN-like mass-loss episodes, exposing the ^{18}O -rich material. Clayton et al. (2005), armed with the detection of a high ^{18}O abundance in one HdC star, HD 137613, and using current information about nuclear reaction rates and stellar interiors, discussed the nucleosynthesis that could possibly lead to the unusual oxygen and carbon isotopic abundance ratios in an isolated intermediate mass star. They noted that the only evolutionary phase that is able to produce the observed oxygen isotopic ratio as well as satisfy the elemental abundance constraints for He and CNO, occurs at the onset of He-burning after completion of H-burning, via the same α -capture reaction as above. For example, in early-AGB stars the ^{18}O enhancement is found only in a thin layer of the He-burning shell. Clayton et al. (2005) speculated that HD 137613 may be a peculiar object that has somehow managed to strip all of its envelope material precisely down to the narrow

layer where the observed extremely low value of $^{16}\text{O}/^{18}\text{O}$ is found.

However, the observations reported here demonstrate that an extreme excess of ^{18}O is a common and possibly universal feature of HdC and RCB stars. Even if the above α -capture reaction is the source of the enhanced ^{18}O , the idea that for a large set of stars post-AGB mass loss proceeds nearly precisely to the ^{18}O -enriched layer and then stops is highly improbable. Another mechanism must be the cause of the enhancement. Moreover, the uniquely low values of $^{16}\text{O}/^{18}\text{O}$ in HdC and RCB stars make it obvious that these two classes of carbon-rich and hydrogen-poor objects are indeed closely related. Therefore, we suspect that the isotopic ratios are an important clue in determining the formation pathway of HdC and RCB stars in general.

Recent studies of V605 Aql and Sakurai’s Object imply that a FF origin for most of the RCB and HdC stars is unlikely (Clayton et al. 2006), based, for example, on the short time that FF stars spend in the region of the HR diagram where RCB stars are found. Although Sakurai’s Object, as a certain representative of the FF scenario, shares a number of characteristics with the RCB stars, there are some important differences (Asplund et al. 1998, 1999, 2000). Its abundances resemble V854 Cen and the other minority-class RCB stars (Asplund et al. 1998). However, in Sakurai’s Object and probably in V605 Aql, $^{12}\text{C}/^{13}\text{C}$ is low indicating efficient H-burning, while in the RCB and HdC stars it is generally high, thereby excluding the possibility that we are seeing material processed by efficient H-burning (Clayton et al. 2006). Moreover, infrared spectra of Sakurai’s Object obtained during 1997–1998 when it had strong CO overtone bands showed no evidence for $^{12}\text{C}^{18}\text{O}$ (Geballe et al. 2002). Therefore, Sakurai’s Object and the other FF stars on the one hand, and most of the RCB and HdC stars on the other hand, are likely to be stars with different origins.

As we have discussed before, ^{18}O can be overproduced in an environment of partial He-burning in which the temperature and the duration of nucleosynthesis are such that the $^{14}\text{N}(\alpha, \gamma)^{18}\text{F}(\beta^+)^{18}\text{O}$ reaction chain can produce ^{18}O , if the ^{18}O is not further processed by $^{18}\text{O}(\alpha, \gamma)^{22}\text{Ne}$. This has also been suggested by Lambert (1986)². Current understanding of mixing and nucleosynthesis events in the FF scenario, which leads to predictions in excellent agreement with Sakurai’s Object (Alcock et al. 2001), is that the surface abundance after the FF is dominated by the intershell material, possibly with the superposed signature of H-ingestion nucleosynthesis if the FF was a VLTP. In the He-shell flash ^{14}N is completely burned into ^{22}Ne as temperatures are so high that ^{18}O is destroyed. In the case of a VLTP, however,

²However, it should be noted that two of the RCB stars, V3795 Sgr and Y Mus, as well as the extreme helium (EHe) stars, show high $[\text{Ne}/\text{Fe}]$ ratios (Asplund et al. 2000). These stars are too hot to show CO bands so nothing is known about their ^{18}O abundances.

there is additional nucleosynthesis due to the ingestion of H-rich envelope material into the He-shell flash convection zone. This may separate the upper H-flash driven convection zone from the original He-shell flash convection zone. In the upper convection zone, He-burning will be terminated and one needs to consider if conditions for ^{18}O overproduction exist there. However, p-capture nucleosynthesis, induced by the H-ingestion event, efficiently destroys ^{18}O and therefore we do not predict any overabundance of ^{18}O in the FF case. It should be mentioned though that the FF scenario involves complicated, hydrodynamic mixing events that may violate some of the assumptions made in 1-D stellar evolution. We cannot, therefore, conclusively settle this question at present.

The above difficulties in producing an extreme ^{18}O excess together with concerns about the ability of FF events to account for the observed number of RCB and HdC stars have led us to explore an alternative evolutionary origin for the RCB and HdC stars, namely that of DD mergers. In particular we have considered the onset of He-burning nucleosynthesis in a He-WD/CO-WD merger. Webbink (1984) proposed that an RCB star evolves from the merger of a He-WD and a CO-WD which has passed through a common envelope phase. He suggested that as the binary begins to coalesce because of the loss of angular momentum by gravitational wave radiation, the (lower mass) He-WD is disrupted. A fraction of the helium is accreted onto the CO-WD and starts to burn, while the remainder forms an extended envelope around the CO-WD. This structure, a star with a helium-burning shell surrounded by a $\sim 100 R_{\odot}$ hydrogen-deficient envelope, would resemble that of an RCB star (Clayton 1996). The merging times ($\sim 10^9$ yr) might not be as long as previously thought, which makes the DD scenario an appealing alternative to the FF scenario for the formation of RCB stars (Iben et al. 1997, 1996). In addition, Saio & Jeffery (2002) suggested that a WD-WD merger could also account for the elemental abundances seen in RCB stars. Pandey et al. (2006) have suggested a similar origin for the EHe stars.

In order to judge the viability of this scenario in the light of our new observations, and in order to determine the direction of future more laborious and detailed modeling efforts we have investigated two separate questions in parallel. We have analyzed the thermodynamic conditions during the dynamic merger process of the two WDs (Section 5.1), and we have investigated the necessary conditions to generate the observed abundance patterns from a nucleosynthetic point of view (Section 5.2). As we show in this section, these two approaches give compatible results, thereby boosting our confidence that the new observations will eventually be fully explainable in the WD merger scenario.

5.1. The Double Degenerate Merger

The purpose of this section is to determine the thermodynamic conditions encountered during the dynamic merger process of a He- and a CO-WD. We discuss first the conditions that lead to complete, dynamical tidal disruption of the He-WD, which is the scenario in which the large overproduction of ^{18}O may be possible. The critical parameter is the mass of the He-WD. After discussing the conditions for tidal disruption, we examine the thermodynamic conditions during disk accretion to determine if they allow the types of nucleosynthesis that might result in the observed overproduction of ^{18}O .

5.1.1. Tidal Disruption

To determine the extent and structure of the disk formed in the merger, we must examine the merger evolution. The merger process begins when the He-WD is brought so close to its companion (either by magnetic braking or gravitational wave emission) that it overfills its Roche radius. The orbital separation at which a WD of this radius will overfill its Roche radius is given by Eggleton (1983):

$$A_0 = R_{\text{He}} \frac{0.6q^{2/3} + \ln(1 + q^{1/3})}{0.49q^{2/3}}, \quad (1)$$

where $q = M_{\text{He}}/M_{\text{CO}}$ with M_{CO} equal to the mass of the CO-WD and M_{He} , R_{He} are set to the mass and radius of the He-WD, respectively. Assuming a $\Gamma = 5/3$ polytrope approximation of a WD equation of state, we derive an equation for the radius of the He-WD (Nauenberg 1972):

$$R_{\text{He}} = 10^4 (M_{\text{He}}/0.7M_{\odot})^{-1/3} [1 - M_{\text{He}}/M_{\text{Ch}}]^{1/2} (\mu_e/2)^{-5/3} \text{km}, \quad (2)$$

where $M_{\text{Ch}} \approx 1.4$ is the Chandrasekhar mass and μ_e is the mean molecular weight per electron of the WD.

As matter flows from the He-WD onto a disk around its companion, both the Roche-overflow radius of the WD and the orbital separation of the binary change. The degenerate nature of the He-WD causes it to expand as it loses mass. If orbital angular momentum were conserved, the orbital separation would also increase as the low-mass He-WD accretes onto its heavier companion. The accretion process could then follow one of two possible paths: the He-WD radius increases faster than the orbital separation and the WD is disrupted over the course of one or two orbital periods, or the orbital separation increases faster than the WD radius and the He-WD accretes onto its companion on a timescale set by magnetic braking. To determine the path our objects follow, we compare the expansion of both the He-WD and the binary separation.

However, orbital angular momentum is not conserved; a fraction of it is transferred into angular momentum of the disk. Assuming no mass is ejected, the angular momentum as a function of the evolving WD mass is (Fryer et al. 1999; Podsiadlowski et al. 1992):

$$\frac{A}{A_0} = \left(\frac{M_{\text{He}}}{M_{\text{He}}^0} \right)^{C_1} \left(\frac{M_{\text{CO}}}{M_{\text{CO}}^0} \right)^{C_2}, \quad (3)$$

where $C_1 \equiv -2 + 2j_{\text{disk}}$ and $C_2 \equiv -2 - 2j_{\text{disk}}$ and j_{disk} is the specific angular momentum of the accretion disk material (see Fryer et al. 1999, for details). Fryer et al. (1999) found for the case of WD-black hole mergers that more than half of the angular momentum in the accreting material found its way into the disk or into the black hole spin (that is, $j_{\text{disk}} \gtrsim 0.5$). It is likely the larger disks produced by these low-mass WD mergers will carry even more angular momentum.

The orbital separation as a function of He-star mass for four separate binary systems is shown in Fig. 3. The solid curves show the path we expect the binaries to follow as the He-star loses mass (going right to left in decreasing He-star mass). The four curves denote four different values of j_{disk} . The dotted curve shows the separation for Roche-lobe overflow for this binary (again, a function of the He-star mass). There are two things to note in this figure. First, if $j_{\text{disk}} > 0.5$, the separation of the binary system will always be less than the separation for Roche-lobe overflow until the star is disrupted ($\sim 0.1 M_{\odot}$). This means that when the WD starts accreting, it will not stop until the companion WD is completely disrupted. The accretion process should proceed on a few orbit timescale: ~ 1000 s. Second, the orbital separation does not increase significantly during this accretion process for such high values of j_{disk} . Tidal effects will send some material as far out as twice the initial separation (but very little will be ejected - see Fryer et al. (1999)). But the bulk of the accreting material will not span more than twice the initial orbital separation at the onset of Roche-lobe overflow.

5.1.2. Disk Accretion

Based on WD merger calculations by Fryer et al. (1999), we expect most of the matter in the He-WD to accrete onto its CO-WD companion. The He-WD is disrupted nearly instantaneously, forming a disk with a total radius of nearly 2 times the separation at the onset of Roche-lobe overflow. The accretion rate onto the CO-WD will definitely vary with time, but to obtain a preliminary estimate of it and of the temperature, we calculate the average value for these quantities.

Under the α disk prescription for transporting angular momentum in the disk formed by the WD disruption, we can estimate the accretion time: $t_{\text{acc}} = P_{\text{disk}}/\alpha$ where P_{disk} is

the orbital period of the disk and α is the viscosity of the disk. Fig. 4 shows this accretion time as a function of the mass of the CO-WD assuming $\alpha = 10^{-3}$. The corresponding mass accretion rate (\dot{M}_{acc}), roughly $M_{\text{He}}/t_{\text{acc}}$, is also plotted in Fig. 4. The entire disk is likely to accrete in a few days, with accretion rates as high as $150 M_{\odot} \text{ yr}^{-1}$.

If this material accreted in a steady system, it would build up an atmosphere on the WD. Accretion atmospheres have been studied in detail for the case of neutron stars (Chevalier 1989; Fryer et al. 1996; Colgate et al. 1993). Fryer et al. (1996) derived the entropy, S , of this atmosphere as a function of the compact remnant mass, in this case, the WD mass (M_{WD}), position of shock (r_{shock})³, and the accretion rate (\dot{M}_{acc}). The pressure of this accreting material will be nearly dominated by photons. For a $\gamma = 4/3$, radiation dominated gas, the entropy is given by:

$$S = 27.9 M_{\text{WD}}^{7/8} \dot{M}_{\text{acc}}^{-1/4} r_{\text{shock}}^{-3/8} \quad (4)$$

where the M_{WD} is in M_{\odot} , \dot{M}_{acc} is in $M_{\odot} \text{ yr}^{-1}$ and r_{shock} is in 10^{10} cm . As the atmosphere builds, the entropy at higher layers will decrease, and this negative entropy gradient will lead to rapid convection, producing a flatter entropy profile on timescales inversely proportional to the Brunt-Väisälä frequency, roughly 1-100 s. But the extent of this atmosphere, and hence, the lower limit on the entropy, is difficult to determine without actual calculations (indeed, given the dynamic nature of this accretion, such a simple picture may not even be correct). Typical initial entropies are roughly 10-30 erg K^{-1} for this accreting atmosphere, but it is possible that the convection can drive the value down by a factor of ~ 2 . We can derive a temperature and a density of the atmosphere as a function of entropy:

$$T = 2.262 \times 10^8 S^{-1} (R/10^{10} \text{ cm})^{-1} \text{K}, \quad (5)$$

and

$$\rho = 390 (S/10 \text{ k}_B \text{ nucleon}^{-1})^{-4} (R_{\text{CO}}/10^9 \text{ cm})^{-3} \text{g cm}^{-3}. \quad (6)$$

The corresponding temperature for the atmosphere at the surface of the CO-WD lies in the $1 - 2 \times 10^8 \text{ K}$ range if we assume the highest value for the entropy. The temperature could increase if mixing brings lower entropy material down, but is likely not to exceed $4 \times 10^8 \text{ K}$. The high temperatures and short dynamic nature of the merger process are supported by multi-dimensional SPH simulations as well (Guerrero et al. 2004).

³This is initially the CO-WD radius but it may move outward an order of magnitude

5.2. Implications from Nucleosynthesis

Now that we have a rough physical picture of the merger process and the corresponding thermodynamic conditions we turn to the nucleosynthesis part of the problem. We ask what conditions are required for nucleosynthesis to produce the observed abundances.

5.2.1. *Observational Signatures of HdC and RCB Stars*

Typical RCB abundances are characterized by extreme hydrogen deficiency, enrichment relative to Fe, of N, Al, Na, Si, S, Ni, the s-process elements and sometimes O (Lambert 1986; Asplund et al. 2000). Based on their abundance characteristics, RCB stars can be divided into a homogeneous majority and a diverse minority class, the latter distinguished by, among other things, lower metallicity, generally less striking H-deficiency, and extreme abundance ratios such as Si/Fe and S/Fe (Asplund et al. 2000). The isotopic carbon ratio, $^{12}\text{C}/^{13}\text{C}$, where measured, is very large (> 500) in most RCB stars. One exception is the minority-class RCB, V CrA, where $^{12}\text{C}/^{13}\text{C}$ is estimated to be between 4 and 10 (Rao 2005). The elemental abundances of the HdC stars are similar to those of the majority of RCB stars (Warner 1967; Asplund et al. 1997; Kipper 2002). Lithium is seen in four of the majority-class RCB stars and at least one HdC star, HD 148839 (Rao & Lambert 1996). Also, although difficult to estimate, C/He is believed to be high in both classes of stars ($\sim 1\text{-}10\%$, Asplund et al. 2000).

The surface compositions of HdC and RCB stars are extremely He-rich (mass fraction 0.98), indicating that the surface material has been processed through H-burning. After H-burning via the CNO cycle, N is by far the most abundant of the CNO elements, because ^{14}N has the smallest nuclear p-capture cross-section of any stable CNO isotope involved. However, the majority of RCB stars has $\log C/N = 0.3^4$ and $\log N/O = 0.4$ by number, equivalent to mass ratios of $C/N = 1.7$ and $N/O = 2.2$ (Asplund et al. 2000). The N/O ratio represents the average for the majority RCB stars although the individual stars show a large scatter. Thus C is the most abundant and O the least abundant CNO element. These abundances are consistent if the material at the surfaces of HdC and RCB stars experienced a small amount of He-burning, as for example at the onset of a He-burning event that is quickly terminated. This partial He-burning would not significantly deplete He, but could be sufficient for some of the ^{14}N to be processed into ^{18}O . At the onset of He-burning, ^{13}C is

⁴There is still an unresolved C-problem in the spectral abundance analysis. The value, $\log C/N = 0.3$, for the majority RCB stars is only true if the derived C abundance rather than the input C abundance is adopted, which rather would give $\log C/N = 0.9$ (Asplund et al. 2000).

the first α -capture reaction to be activated because of the large cross-section of $^{13}\text{C}(\alpha, n)^{16}\text{O}$. Thus, a large $^{12}\text{C}/^{13}\text{C}$ ratio and enhanced s-process elements are both consistent with partial He-burning.

5.2.2. Parametric Nucleosynthesis Model

We constructed a parametric nucleosynthesis model for a quantitative estimate of the partial He-burning nucleosynthesis scenario (Fig. 5). We consider a single zone nucleosynthesis calculation with a solar initial abundance distribution. The density is assumed to be $2 \times 10^3 \text{ g cm}^{-3}$ and the temperature initially is $5 \times 10^7 \text{ K}$. We follow the nucleosynthesis with a nuclear network code until the H has been burned to a mass fraction $< 10^{-4}$. This situation is reached after approximately 125 yr. This first phase in our model represents H-burning, e.g., in the core or in a shell, that produces the He in the He-WD. The assumed density is unrealistically high, because, for simplicity we do not adjust the density in different phases of the model. In practice, varying the density will only affect the timescale associated with each burning phase. Here, the first phase serves only one purpose: to easily arrive at an abundance distribution that reflects that in a He-WD.

At the end of the H-burning phase, we increase the temperature to switch smoothly into the He-burning regime (Fig. 5). In our scenario, this temperature rise will occur as a result of the accretion of the He-WD onto the more massive CO-WD. Here we assume a temperature rise of $1\% \text{ yr}^{-1}$. The timescale is not important here as everything scales with the density. The purpose is only to see how the relative abundances change as a function of temperature.

We stop the increase when $T = 1.65 \times 10^8 \text{ K}$, which occurs at $\approx 245 \text{ yr}$. For even slightly larger maximum temperatures, He-burning quickly reduces the abundances of He and ^{14}N to much smaller values than observed in the HdC and RCB stars. Lower temperatures require a much longer time for ^{14}N to be transformed into ^{18}O . From the merger considerations in the previous section, we anticipate that the period of He-burning cannot be very long if it is a result of the dynamical merging process. The exact timescale depends on the density evolution. After stopping the temperature increase, we allowed the network to continue for another 255 yr until abundances are reached that clearly disagree with those seen in the HdC and RCB stars.

5.2.3. Results

Fig. 5 (upper right panel) shows the evolution of the dominant CNO isotopes. Initially the CNO H-burning equilibrium ratios, including the large ^{14}N abundance are established. Then, as the temperature increases, a modest increase in the ^{16}O abundance can be seen (at 220 yr), resulting from the activation of $^{13}\text{C}(\alpha, n)^{16}\text{O}$. Thereafter ^{16}O remains largely unchanged because the temperature does not become high enough for $^{12}\text{C}(\alpha, \gamma)^{16}\text{O}$. However, just after ^{13}C burning, ^{14}N begins undergoing α -capture, producing ^{18}O . This reaction very quickly makes ^{18}O the most abundant of the CNO isotopes, a situation that lasts until ^{18}O begins capturing α particles to produce ^{22}Ne at which time it is overtaken by ^{12}C whose abundance has been increasing since $t = 230$ yr because of the triple- α reaction.

The evolution of the elemental C/N and N/O ratios (lower left panel) is qualitatively consistent with nucleosynthesis after full completion of H-burning and at the beginning of He-burning. The N/O ratio decreases when the temperature is high enough to start He-burning, and eventually reaches the mean observed value at ~ 250 yr. The C/N ratio increases, but reaches the observed mean value somewhat later. However, both times are consistent with a very high and only slightly decreased He abundance at this early time of He-burning.

The most pertinent information in Fig. 5 is the evolution of the $^{16}\text{O}/^{18}\text{O}$ and $^{12}\text{C}/^{13}\text{C}$ ratios (lower right panel). The enormous production of ^{18}O from ^{14}N leads to a rapid decrease of the $^{16}\text{O}/^{18}\text{O}$ ratio at the onset of He-burning, which passes through the observed value for HD 137613 at around 250 yr. The $^{12}\text{C}/^{13}\text{C}$ ratio increases to the point that it exceeds its observed lower limit of 500 (Fujita & Tsuji 1977) at a slightly earlier time.

5.2.4. Admixture of H

It is intriguing that most of the observed abundances of the HdC and RCB stars that have been discussed so far seem consistent with a nucleosynthetic origin at the onset of He-burning. One must keep in mind that this simulation consists of only a single zone, and that the temperature evolution is roughly assumed to demonstrate the various stages of nucleosynthesis in a DD merger. Nevertheless, one may complain that the two observations are not well matched. The C/N ratio increases too late, when $^{16}\text{O}/^{18}\text{O}$ and N/O have already reached values far from those observed. The other inconsistency is the observed enhancement of s-process elements. In our model, the only source of neutrons is the small amount of ^{13}C from H-burning via the CNO cycle. This is insufficient by far to produce significant s-process enhancements. In addition, a good match for the CNO elemental and isotopic abundances is only obtained for a short period. Possibly the observed values are the result of a characteristic

termination timescale for this process and the associated nucleosynthesis. The admixture of H could lead to an enrichment of ^{14}N (Rao & Lambert 1996; Asplund et al. 2000).

However, the CO-WD retains a small H-rich envelope, 10^{-3} - $10^{-4} M_{\odot}$ depending on the WD mass. The accreting material will be shocked and heated, quickly leading to violent He-burning, which will induce convection. In addition, the accreted layer will be perturbed by the ongoing dynamic merging phase. All this will help to bring the original H-rich WD envelope up into the accreted He-burning material. In particular, the fact that the accreted elements have larger atomic masses make mixing of the H-rich CO-WD envelope into the accreted He-rich material inevitable.

The question is when and how much H-rich material will be added. With our one-zone model we can only crudely explore the effect of such an H-admixture. In reality, there will be multi-zone mixing and burning at a range of densities and temperatures. Nevertheless, if the temperatures of the hottest layers are about right, one can obtain a zeroth-order approximation to what really happens. The admixture of a substantial fraction of the H-rich CO-WD envelope has to occur at a time when some ^{12}C has already been produced through He-burning, because a significant new source of ^{12}C is required for additional p-captures to produce the ^{13}C that can serve as a neutron source for the s-process. From Fig. 5, it is clear that triple- α reactions are only activated at a temperature of $1.6 \times 10^8 \text{ K}$ at the assumed density. Then, the admixture must occur after that temperature has been reached.

To test these ideas, we selected a CO-WD envelope mixture to be blended into the He-burning accreted material. The mixture comes from an actual post-AGB stellar evolution calculation with a core mass of $0.6 M_{\odot}$ and an initial ZAMS mass of $2 M_{\odot}$. It has enhanced ^{12}C ($X_{\text{C}} = 1.4 \times 10^{-2}$) and ^{16}O ($X_{\text{O}} = 1.5 \times 10^{-2}$), considerably larger than our initial choice of solar abundances ($X_{\text{C}} = 3 \times 10^{-3}$, $X_{\text{O}} = 8.3 \times 10^{-3}$) due to several third dredge-up events during the TP-AGB evolution phase preceding the WD formation. The accreted He-WD material has a mass of order $0.1 M_{\odot}$, while the CO-WD envelope has a mass of the order $5 \times 10^{-4} M_{\odot}$. Thus, we admix the envelope in a ratio 1:0.005 and renormalize to unity. We examine the effect of this admixture at the time when the ^{12}C abundance reaches a mass fraction of 5×10^{-3} .

Fig. 6 shows the results of the network calculation. As the H-rich material is admixed at this early stage of He-burning, it encounters a large ^{18}O abundance. Through two successive p-captures, $^{18}\text{O}(\text{p}, \alpha)^{15}\text{N}(\text{p}, \alpha)^{12}\text{C}$, most of the ^{18}O is transformed into ^{12}C . ^{19}F is formed by $^{18}\text{O}(\text{p}, \gamma)^{19}\text{F}$ and, because of the large abundance of ^4He also through $^{15}\text{N}(\alpha, \gamma)^{19}\text{F}$. Temporarily, the ^{19}F abundance exceeds the solar value by two orders of magnitude. We note that lines of F I were recently detected for the first time in visible spectra of a group of extreme He stars (Pandey 2006). The ^{12}C nuclei, both freshly produced from triple- α

(primary), and coming from ^{18}O make ^{13}C in turn producing neutrons and ^{16}O through α -capture: $^{12}\text{C}(\text{p}, \gamma)^{13}\text{N}(\beta^+)^{13}\text{C}(\alpha, \text{n})^{16}\text{O}$.

Due to the burning of ^{13}C , the ^{16}O abundance is increasing quickly. The abundance of ^{14}N also increases because of $^{13}\text{C}(\text{p}, \gamma)^{14}\text{N}$. The admixture takes place just after the C/N ratio has increased significantly above the observed mean value. Due to the burning of ^{12}C and the creation of ^{14}N , the C/N ratio drops below the observed value again. The opposite happens to the N/O ratio. At the time of the admixture, ^{18}O dominates the O elemental abundance. Its quick decrease plus the increase in ^{14}N lead to a rapid increase in the N/O ratio above the observed ratio.

The effects of the admixture on the $^{12}\text{C}/^{13}\text{C}$ and $^{16}\text{O}/^{18}\text{O}$ ratios are dramatic. Due to the burning of ^{18}O and the increase in ^{16}O from the $^{13}\text{C}(\alpha, \text{n})^{16}\text{O}$ reaction, the $^{16}\text{O}/^{18}\text{O}$ ratio quickly rises beyond the observed values. The $^{12}\text{C}/^{13}\text{C}$ ratio decreases, partly due to the admixture of ^{13}C from the CO-WD envelope (the first jump down to $\log^{12}\text{C}/^{13}\text{C} \approx 4$) and then partly due to the production of ^{13}C from $^{12}\text{C}(\text{p}, \gamma)$.

The effect on s-process elemental abundances should also be profound. Due to the production of the ^{13}C at high He-burning temperatures, neutrons are rapidly released. In this particular admixture test, we find $\tau_{\text{exp}} = 0.13 \text{ mbarn}^{-1}$ and a peak neutron density of $N_{\text{n}} > 10^{11} \text{ cm}^{-3}$. Thus, the neutron exposure is in the range that could explain the observed s-process elements (Asplund et al. 2000). However, the neutron density is far too high to produce an s-process signature.

In summary, it seems that the admixture of H can aid in solving the delay in the match of the elemental and isotopic ratios. It also has, in general, the effect of reversing the effect of too much He-burning. For example, the He-burning leads to the decrease of $^{16}\text{O}/^{18}\text{O}$ to values far below the lowest observed. H-admixture has the effect of reversing this trend and increasing the O isotopic ratio again. The same can be observed for the other abundance ratios. We therefore speculate that H-admixture in a realistic, highly mixed accretion environment can help to stabilize the nucleosynthesis results leading to the significant coherence of abundance patterns observed in HdC and RCB stars.

6. Conclusions

Observations of the first overtone CO bands in cool HdC and RCB stars have resulted in two significant findings: (1) in all HdC stars and most or all RCB stars where oxygen isotopic ratios can be measured, ^{18}O is enhanced relative to ^{16}O by factors of 100–1000 compared to standard Galactic values; and (2) the lowest $^{16}\text{O}/^{18}\text{O}$ ratios are found in the

HdC stars. Our models show that nucleosynthesis in the dynamically accreting material of CO-WD–He-WD mergers, previously suggested as the source of RCB stars, may provide a suitable environment for significant production of ^{18}O and the very low $^{16}\text{O}/^{18}\text{O}$ values as observed. The suggestion that FF events produce RCB stars appears to be weakened due to a mismatch of oxygen (this paper) and carbon isotopic abundances, as well as by the apparent inconsistency in timescale of the RCB-mimicking portion of the FF episode and that required to account for the number of RCB stars (Clayton et al. 2006). Therefore, we have explored the idea that HdC and RCB stars originate in the mergers of CO- and He-WDs.

In the WD merger, it is partial He-burning at just the right temperature and duration that is the likely generator of small $^{16}\text{O}/^{18}\text{O}$ ratios. In addition, the high values of $^{12}\text{C}/^{13}\text{C}$ observed in HdC and RCB stars can probably be reproduced at the same time. The observed s-process abundances in these stars as well as the delayed increase of the C/N ratio to the observed mean value motivated the investigation of the effects of admixing H-rich material. This material would, in the DD merger/accretion scenario, be the thin CO-WD envelope. We found that qualitatively the instantaneous admixture of H-rich material resets all observables back toward the observed values. The fact that all of the H-rich material is added instantaneously leads to artefacts such as the extremely large neutron density, as well as the very small $^{12}\text{C}/^{13}\text{C}$ ratio. In reality, the admixture will take place over a finite time and in smaller quantities. A slower rate of admixing could produce the observed abundances.

It is interesting to note that some RCB stars show enhanced Li abundances, as does the FF star Sakurai’s Object (Lambert 1986; Asplund et al. 1998). As shown by Herwig & Langer (2001), Li enhancements are consistent with the FF scenario. However, the production of ^{18}O requires temperatures large enough to at least marginally activate the $^{14}\text{N}(\alpha, \gamma)$ reaction. The α capture on Li is eight orders of magnitude more effective than on ^{14}N . For that reason the simultaneous enrichment of Li and ^{18}O is not expected in the WD merger scenario. This is an important argument against the FF evolution scenario as a progenitor of RCB and HdC stars with excess of ^{18}O . The presence of Li in some RCB stars, as well as in Sakurai’s Object, is extremely difficult to explain with a WD merger. Since ^{18}O strongly supports the DD merger/accretion scenario for most of the stars studied so far, the obvious solution is that there are (at least) two evolutionary channels leading to RCB, HdC and EHe stars, perhaps with the DD being the dominant mechanism. Unfortunately the division between majority- and minority-class RCB stars does not lend itself naturally to this explanation, since Li has only been detected in the majority group (Asplund et al. 2000).

Contrary to the work of Saio & Jeffery (2002), who assumed an accretion rate of $10^{-5} M_{\odot}/\text{yr}$ to model WD mergers with a hydrostatic evolution code, our estimate of the merger process

leads to a picture of a rapid, dynamic event that only lasts a few days, and during which high temperatures can be obtained. In the merger scenario, rapidity appears to be essential to producing the conditions required to account for our observations of extremely abundant ^{18}O .

Understanding the RCB and HdC stars is a key test for any theory that aims to explain hydrogen deficiency in post-AGB stars. Confirmation of the WD merger scenario will allow the use of RCB and HdC stars as probes for WD merger simulations. The ability to model the rates of these low-mass WD mergers will help us to understand the rates of more massive mergers that make type Ia supernovae (Belczynski et al. 2005).

Most of these observations were obtained during program GS-2005B-Q-20 at the Gemini Observatory, which is operated by AURA under a cooperative agreement with the NSF on behalf of the Gemini partnership of Argentina, Australia, Brazil, Canada, Chile, the United Kingdom and the United States of America. We are indebted to the Gemini staff for its expertise in obtaining these data. We also thank the staff of UKIRT, which is operated by the Joint Astronomy Centre on behalf of the U.K. Particle Physics and Astronomy Research Council. TRG’s research is supported by the Gemini Observatory, which is operated by the Association of Universities for Research in Astronomy, Inc., on behalf of the international Gemini Partnership. This work was carried out in part under the auspices of the National Nuclear Security Administration of the U.S. Department of Energy at Los Alamos National Laboratory under Contract No. DE-AC52-06NA25396, and funded by the LDRD program (20060357ER). This work is LANL report LA-UR-07-0198. This work was carried out in part in collaboration with the NSF funded Joint Institute for Nuclear Astrophysics (JINA).

REFERENCES

- Alcock, C., Allsman, R. A., Alves, D. R., Axelrod, T. S., Becker, A., Bennett, D. P., Clayton, G. C., Cook, K. H., Dalal, N., Drake, A. J., Freeman, K. C., Geha, M., Gordon, K. D., Griest, K., Kilkenney, D., Lehner, M. J., Marshall, S. L., Minniti, D., Misselt, K. A., Nelson, C. A., Peterson, B. A., Popowski, P., Pratt, M. R., Quinn, P. J., Stubbs, C. W., Sutherland, W., Tomaney, A., Vandehei, T., & Welch, D. L. 2001, *ApJ*, 554, 298
- Amari, S., Zinner, E., & Lewis, R. S. 1995, *ApJ*, 447, L147
- Asplund, M., Gustafsson, B., Kameswara Rao, N., & Lambert, D. L. 1998, *A&A*, 332, 651
- Asplund, M., Gustafsson, B., Kiselman, D., & Eriksson, K. 1997, *A&A*, 318, 521

- Asplund, M., Gustafsson, B., Lambert, D. L., & Rao, N. K. 2000, *A&A*, 353, 287
- Asplund, M., Lambert, D. L., Kipper, T., Pollacco, D., & Shetrone, M. D. 1999, *A&A*, 343, 507
- Belczynski, K., Bulik, T., & Ruiter, A. J. 2005, *ApJ*, 629, 915
- Bergeat, J., Knapik, A., & Rutily, B. 2001, *A&A*, 369, 178
- Cami, J. & Yamamura, I. 2001, *A&A*, 367, L1
- Chevalier, R. A. 1989, *ApJ*, 346, 847
- Clayton, G. C. 1996, *PASP*, 108, 225
- Clayton, G. C. & De Marco, O. 1997, *AJ*, 114, 2679
- Clayton, G. C., Herwig, F., Geballe, T. R., Asplund, M., Tenenbaum, E. D., Engelbracht, C. W., & Gordon, K. D. 2005, *ApJ*, 623, L141
- Clayton, G. C., Kerber, F., Pirzkal, N., De Marco, O., Crowther, P. A., & Fedrow, J. M. 2006, *ApJ*, 646, L69
- Colgate, S. A., Herant, M., & Benz, W. 1993, *Phys. Rep.*, 227, 157
- Duerbeck, H. W. & Benetti, S. 1996, *ApJ*, 468, L111+
- Duflot, M., Figon, P., & Meyssonier, N. 1995, *A&AS*, 114, 269
- Eggleton, P. P. 1983, *ApJ*, 268, 368
- Ford, H. C. 1971, *ApJ*, 170, 547
- Fryer, C. L., Benz, W., & Herant, M. 1996, *ApJ*, 460, 801
- Fryer, C. L., Woosley, S. E., Herant, M., & Davies, M. B. 1999, *ApJ*, 520, 650
- Fujimoto, M. Y. 1977, *PASJ*, 29, 331
- Fujita, Y. & Tsuji, T. 1977, *PASJ*, 29, 711
- Geballe, T. R., Evans, A., Smalley, B., Tyne, V. H., & Eyres, S. P. S. 2002, *Ap&SS*, 279, 39
- Geiss, J., Gloeckler, G., & Charbonnel, C. 2002, *ApJ*, 578, 862

- Gonzalez, G., Lambert, D. L., Wallerstein, G., Rao, N. K., Smith, V. V., & McCarthy, J. K. 1998, *ApJS*, 114, 133
- Goswami, A., Rao, N. K., Lambert, D. L., & Gonzalez, G. 1997, *PASP*, 109, 796
- Guerrero, J., García-Berro, E., & Isern, J. 2004, *A&A*, 413, 257
- Herwig, F. 2001, *ApJ*, 554, L71
- Herwig, F. & Langer, N. 2001, *Nuclear Physics A*, 688, 221
- Iben, I. J., Tutukov, A. V., & Yungelson, L. R. 1996, *ApJ*, 456, 750
- . 1997, *ApJ*, 475, 291
- Janka, H.-T., Eberl, T., Ruffert, M., & Fryer, C. L. 1999, *ApJ*, 527, L39
- Kipper, T. 2002, *Baltic Astronomy*, 11, 249
- Kraemer, K. E., Sloan, G. C., Wood, P. R., Price, S. D., & Egan, M. P. 2005, *ApJ*, 631, L147
- Lambert, D. L. *ASSL Vol. 128: IAU Colloq. 87: Hydrogen Deficient Stars and Related Objects*, ed. , K. HungerD. Schoenberner & N. Kameswara Rao, 127
- Lawson, W. A. & Cottrell, P. L. 1997, *MNRAS*, 285, 266
- Lawson, W. A., Cottrell, P. L., Kilmartin, P. M., & Gilmore, A. C. 1990, *MNRAS*, 247, 91
- Nauenberg, M. 1972, *ApJ*, 175, 417
- Pandey, G. 2006, *ApJ*, 648, L143
- Pandey, G., Lambert, D. L., Jeffery, C. S., & Rao, N. K. 2006, *ApJ*, 638, 454
- Podsiadlowski, P., Joss, P. C., & Hsu, J. J. L. 1992, *ApJ*, 391, 246
- Ramsay Howat, S. K., Todd, S., Leggett, S., Davis, C., Strachan, M., Borrowman, A., Ellis, M., Elliot, J., Gostick, D., Kackley, R., & Rippa, M. in , *Ground-based Instrumentation for Astronomy*. Edited by Alan F. M. Moorwood and Iye Masanori. *Proceedings of the SPIE*, Volume 5492, pp. 1160-1171 (2004)., ed. A. F. M. MoorwoodM. Iye, 1160–1171
- Rao, N. K. in , *ASP Conf. Ser. 336: Cosmic Abundances as Records of Stellar Evolution and Nucleosynthesis*, ed. T. G. Barnes, IIF. N. Bash, 185–+

- Rao, N. K. & Lambert, D. L. in , ASP Conf. Ser. 96: Hydrogen Deficient Stars, ed. C. S. Jeffery U. Heber, 43
- Renzini, A. 1979, in ASSL Vol. 75: Stars and star systems, ed. B. E. Westerlund, 155–171
- Saio, H. & Jeffery, C. S. 2002, MNRAS, 333, 121
- Scott, P. C., Asplund, M., Grevesse, N., & Sauval, A. J. 2006, A&A, 456, 675
- Tenenbaum, E. D., Clayton, G. C., Asplund, M., Engelbracht, C. W., Gordon, K. D., Hanson, M. M., Rudy, R. J., Lynch, D. K., Mazuk, S., Venturini, C. C., & Puetter, R. C. 2005, AJ, 130, 256
- Warner, B. 1967, MNRAS, 137, 119
- Webbink, R. F. 1984, ApJ, 277, 355
- Wilson, T. L. & Rood, R. 1994, ARA&A, 32, 191
- Zaniewski, A., Clayton, G. C., Welch, D. L., Gordon, K. D., Minniti, D., & Cook, K. H. 2005, AJ, 130, 2293

Table 1. CO Bandhead Absorption Depths in RCB and HdC Stars^a

Star	Tel.	Exp. Time (s)	¹² C ¹⁶ O		¹² C ¹⁸ O	
			2-0	3-1	2-0	3-1
HD 175893	GS	480	0.06	0.07	0.15	0.11
HD 182040	GS	56	0.03	0.05	0.05	0.06
HD 137613	UKIRT	480	0.12	0.20	0.18	0.21
WX CrA	GS	480	0.18	0.20	0.15	0.13
S Aps	GS	160	0.54	0.51	0.26	0.15
SV Sge	GS	80	0.51	0.47	0.24	0.11
ES Aql	GS	480	0.35	0.31	0.09	0.07
Z Umi ^b	Bok	60	0.34	0.34	0.07	0.02
U Aqr	GS	720	0.16	0.24	0.03	<0.02
HD 148839	GS	480	<0.05	<0.03	<0.03	<0.02
HD 173409	GS	960	<0.03	<0.02	<0.02	<0.02

^aBased on flux ratios at rest vacuum wavelengths 2.2930 and 2.2940 μm , 2.3215 and 2.3235 μm , 2.3480 and 2.3495 μm , and 2.3770 and 2.3790 μm for ¹²C¹⁶O 2-0 and 3-1 bands and ¹²C¹⁸O 2-0 and 3-1 bands, respectively.

^bSpectrum originally published by Tenenbaum et al. (2005).

Table 2. Estimated Isotopic Oxygen Abundances

Star	HdC/RCB	T_{eff}	$\text{abs}(\text{C}^{16}\text{O})/\text{abs}(\text{C}^{18}\text{O})$	$^{16}\text{O}/^{18}\text{O}^a$
HD 175893	HdC	5500	0.4	0.2
HD 182040	HdC	5600	0.6	0.3
HD137613	HdC	5400	0.7	0.5
WX CrA	RCB	5300	1.3	1
S Aps	RCB	5400	2.5	4
SV Sge	RCB	4000	2.5	4
ES Aql	RCB	5000	3	6
Z UMi	RCB	5000	≥ 4	≥ 8
U Aqr	RCB	6000	≥ 6	≥ 12
HD 148839	HdC	6500
HD 173409	HdC	6100

^aEstimated uncertainty is a factor of two.

References. — Asplund et al. (1997); Lawson et al. (1990);
Bergeat et al. (2001)

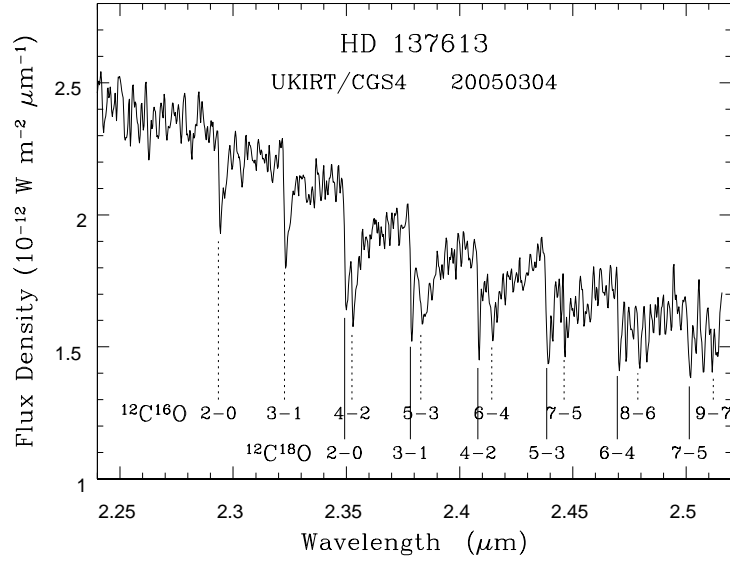


Fig. 1.— UKIRT spectrum of HD 137613. The wavelengths of the bandheads of $^{12}\text{C}^{16}\text{O}$ and $^{12}\text{C}^{18}\text{O}$ are indicated.

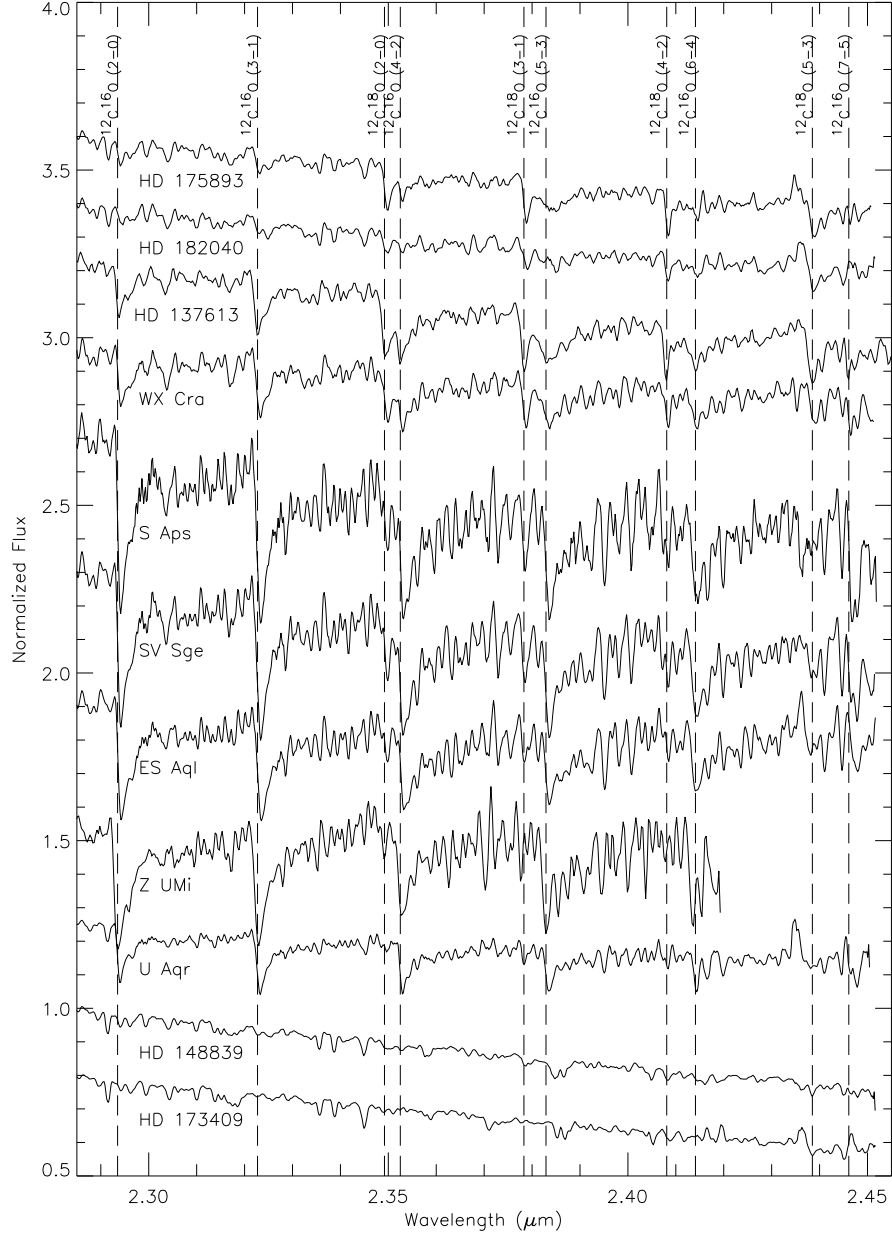


Fig. 2.— 2.28–2.45 μm spectra of RCB and HdC stars, with wavelengths of $^{12}\text{C}^{16}\text{O}$ and $^{12}\text{C}^{18}\text{O}$ bandheads indicated by vertical lines. The stars are ordered by the strengths of the $^{12}\text{C}^{18}\text{O}$ bands. The first three spectra at the top and the last two at the bottom are of HdC stars. The rest are of RCB stars.

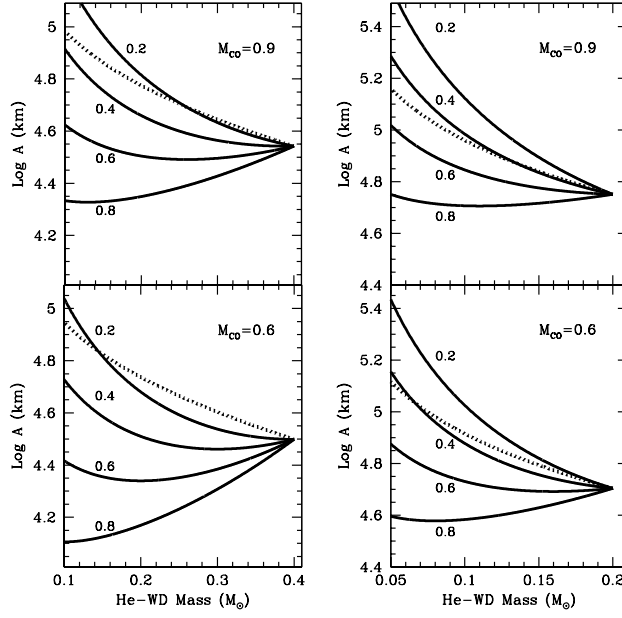


Fig. 3.— Evolution of a WD binary as a function of the masses of the two stellar components. The start of the evolution is where all the lines meet at a point (right side of the plots). The solid lines show the evolution of the orbital separation of the binary as mass transfers from the He-WD onto the CO-WD. The different curves correspond to varying amounts of angular momentum in the disk as a function of the mean binary angular momentum: 0.2 means very little angular momentum goes into the disk, most stays in the binary whereas 0.8 means that the accreting material retains most of its angular momentum as it forms an accretion disk. Models of WD/BH mergers (Fryer et al. 1999) and NS/BH mergers (Janka et al. 1999) all suggest that this number is at least ~ 0.5 . The dotted line denotes the binary separation below which Roche-lobe overflow occurs. Because degeneracy dominates the pressure of the He-WD, as it loses mass, it expands, and the separation at which Roche-lobe overflow occurs also increases. We start the evolution with the orbital separation set to the Roche overflow separation (the onset of Roche-lobe overflow). If the subsequent evolution causes the separation to drop below the Roche overflow separation, the accretion will develop dynamically and will lead to the disruption of the He-WD on an orbital timescale. The four panels correspond to two CO-WD masses (top - $0.9 M_{\odot}$, bottom - $0.6 M_{\odot}$) and two He-WD masses (left - $0.4 M_{\odot}$, right - $0.2 M_{\odot}$).

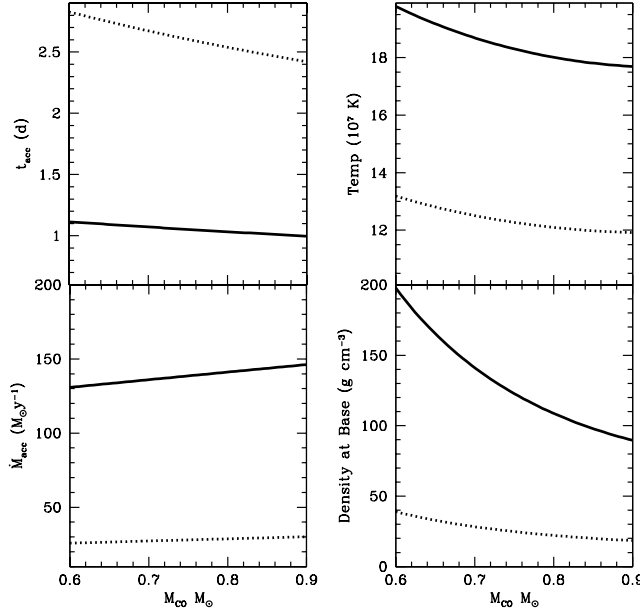


Fig. 4.— Properties of the accretion atmosphere as a function of the C/O mass. The solid and dotted curves correspond to 0.4 and $0.2 M_{\odot}$ He stars, respectively. The top left panel shows the accretion timescale, the bottom left panel shows the corresponding accretion rate. The largest uncertainty for both of these terms is the choice for the viscosity (we have assumed $\alpha \approx 10^{-3}$). This value could be a factor of 100 larger, producing accretion timescales a factor of 100 shorter and accretion rates a factor of 100 larger. If we assume this accretion builds an equilibrium atmosphere on top of the CO-WD, we can then estimate the temperature and density at the base of this atmosphere. This calculation depends upon the size of the atmosphere and also the accretion rate. The latter is the biggest uncertainty and could lead to an increase in the temperature of, at most, a factor of 2, and an increase in the density of roughly a factor of 10. We note, however, that nucleosynthetic constraints argue for our standard calculation.

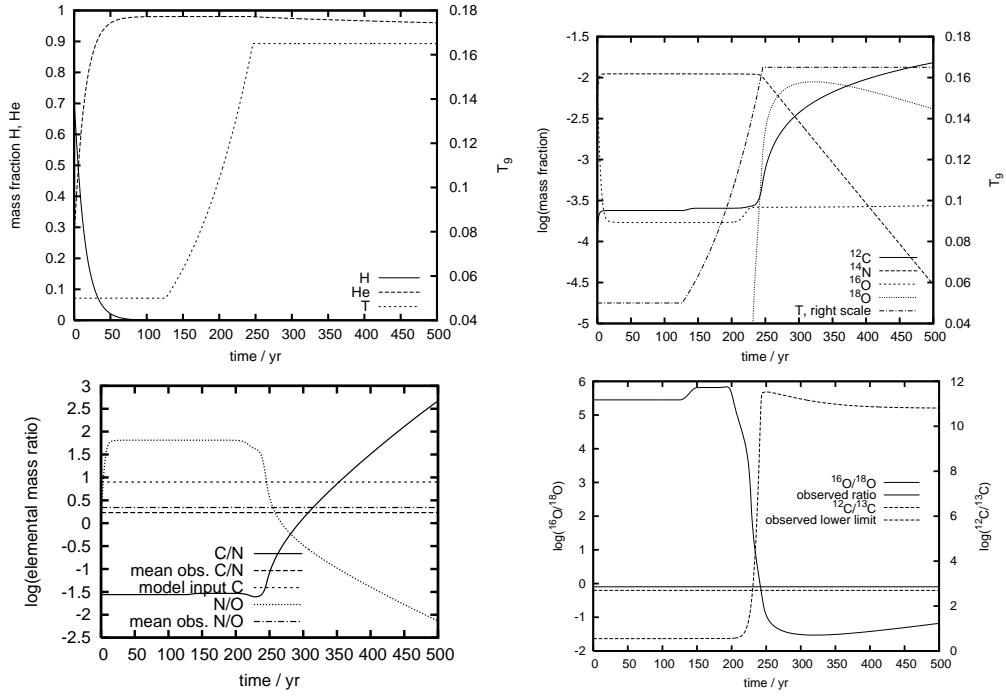


Fig. 5.— Time evolution. Upper left: H and He as well as temperature. Upper right: CNO isotopes, and temperature. Lower left: C/N and N/O ratios and mean observed ratios of majority of RCB stars. Lower right: O and C isotopic ratios and observed ratios (straight lines).

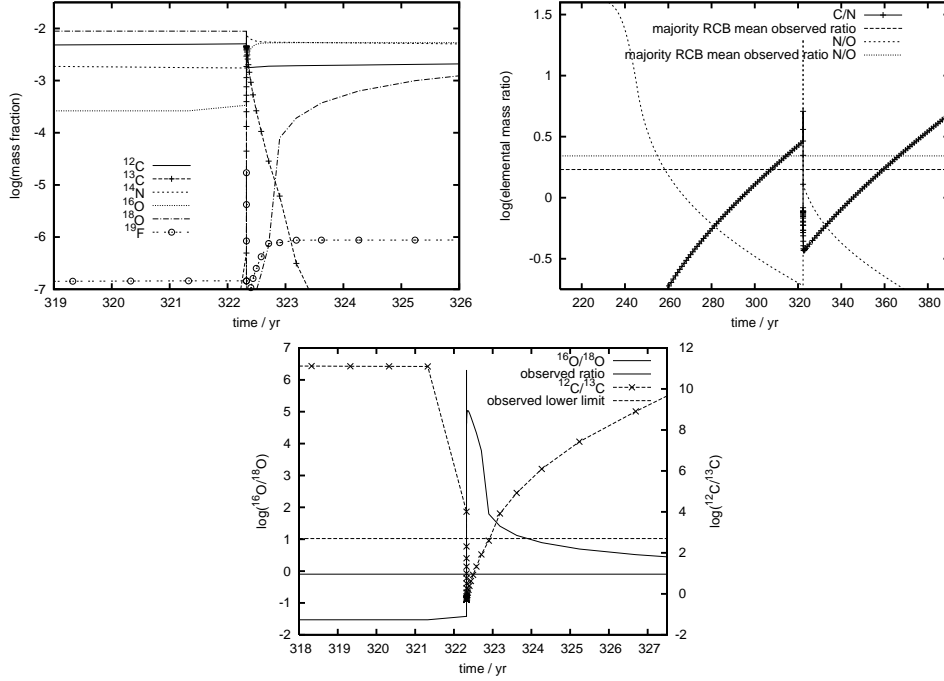


Fig. 6.— Upper left: Same as Fig. 5 for the short period around the time of admixing the H-rich CO-WD envelope material to the He-burning accreting material. Time evolution of CNO isotopes. Each mark along the ^{13}C line represents a time step in the network evolution. Upper right: Time evolution C/N and N/O ratios and mean observed ratios of majority of RCB stars. Lower left: Time evolution of O and C isotopic ratios and observed ratios (straight lines).